CERN Summer 2020 Online learning initiative remote project

Study of the vertexing detector position using material hadronic interaction vertices at the LHCb Upgrade experiment

Maciej Giza

Faculty of Physics, University of Warsaw

Supervisors:
Biljana Mitreska
Lucia Grillo
Silvia Borghi

Abstract

The LHCb experiment is one of the four large experiments at the LHC, designed to perform high precision measurements of CP Violation and rare decays of heavy flavored hadrons. The alignment of the vertexing detector (VELO) is fundamental to achieve the best precision in the reconstruction of primary vertex (defined as the collision point of the two LHC beams) and secondary vertex, where the heavy flavoured hadron decays. The upgraded VELO detector consists of pixel silicon sensors arranged in several modules placed on two retractable halves that close around the interaction region after the LHC beams are declared stable. During physics data taking the VELO modules have the closest approach to the LHC beams among the LHC experiments.

A data-driven method to determine the module position using Monte Carlo events has been studied. In this approach, secondary interactions of hadrons are used to map the location of material in the VELO. This allows to determine, among several elements, the z-position of the modules, which is one of the key elements for a high precision measurement of the decay length of heavy flavoured hadrons. Furthermore, this method makes possible to determine the global position of the VELO and to obtain an independent measurement of the alignment accuracy in data. Precise constraints on the position of the VELO modules are critically important for the high precision programme of the LHCb experiment during the upgrade data taking phase, foreseen to start at the end of 2021.

1 Introduction

The LHCb experiment is a single-arm forward spectrometer dedicated to the study of heavy flavour physics, installed on the Large Hadron Collider (LHC). Its physics program includes precise measurement of CP violation, rare and semileptonic decays of B and D hadrons, study of electroweak and QCD processes, hadron spectroscopy and heavy ion collisions [1], [2]. During the Run 1 of the LHC, the LHCb experiment recorded 3 fb^{-1} of data at center of mass energies 7 and 8 TeV [3] and performed many important measurement in the heavy flavour sector, such as the first observation of the $B_s^0 \to \mu^+\mu^-$ [4] joint with the CMS collaboration, the measurement of a flavour changing neutral current anomaly in the $B^0 \to K^{*0}\mu^+\mu^-$ decay [5], and the observation of pentaquark states [6] in the $\Lambda_b^0 \to J/\psi\ p\ K^-$ decay. LHCb has continued its successful operation during Run 2 (2015–18), during which the increased cross-sections due to the higher collision energy at the center of mass, 13 TeV, and implementation of novel online data processing strategies have led to significant increases in the samples available for analysis [7].

However, numerous crucial measurements have been limited by statistics [8], with experimental precisions not directly comparable to the uncertainties of the theoretical predictions. For this reason, LHCb has undergone a major upgrade during the LHC Long Shutdown 2, that will make it feasible to collect around 50 fb^{-1} of data by 2030 [7].

One of the crucial parts of LHCb is the Vertex Locator (VELO), a tracking detector devoted to track reconstruction and precise measurements of primary and secondary vertices of short living particles. The previous VELO, based on silicon microstrips technology, is replaced by 52 tracking layers based on 50×50 μm^2 pixel technology, ensuring better hit resolution and simpler track reconstruction. The upgraded VELO is closer to the beam axis and the particles will see substantially less detector material before the intersection of tracking layers. Thus the resolution of the measurement of the particles impact parameter will improve, increasing the VELO tracking efficiency, and provide a better decay time resolution [3]. The layout of the detector within the LHCb coordinate system is shown in Figure 1.

It is very similar to the previous VELO layout [1], omitting the fact that the z positions of the modules have been changed in order to optimize the layout in term of acceptance and efficiency. The VELO consists of an array of modules which comprise the tiles with silicon sensors and associated services inside the vacuum. The modules are located in two arrays, the so caled halves, where the left half (A side) is at positive x and the right half (C side) is at negative x.

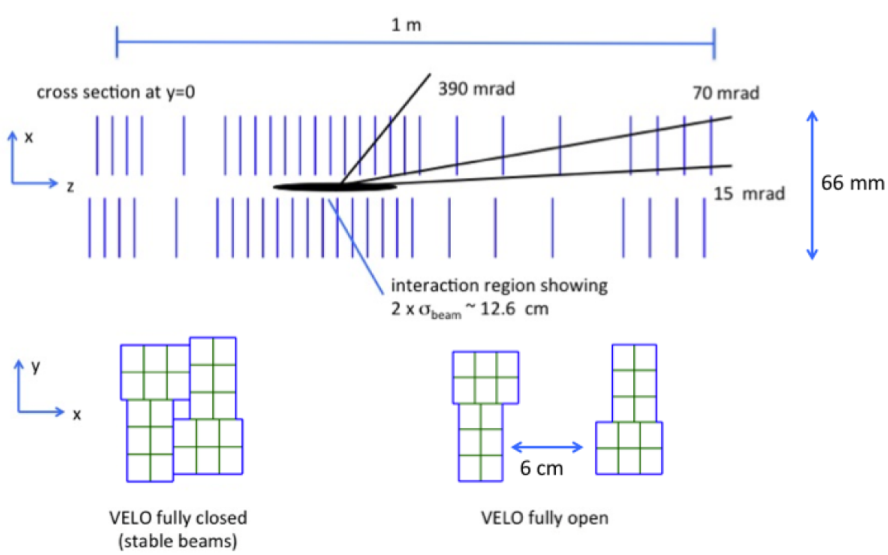

Figure 1: Schematic layout of the upgraded VELO [9]

2 Alignment procedure

The VELO detector is assembled with a high precision with a detailed metrology being performed. However, the only possible method for correcting misalignments of the halves and modules during data taking is through a track-based software alignment procedure. It is based on a method using the Kalman filter [10] track fit which employs a minimum χ^2 algorithm to determine the positions of detector elements (halves, modules and sensors) from a sample of reconstructed tracks and takes into account multiple scattering, energy loss in the material and magnetic field information. The alignment algorithm estimates the misplacement of a set of positions of detector elements with respect to their expected positions [11].

Among possible deformations of modules positions, it is interesting to study the so called "weak modes", i.e. deformations which are difficult - if not impossible - to unfold with tracks. Examples are: global translation or global rotation of the considered detector, shearing and scaling, as shown on the Figure 2.

Due to the VELO geometry, only the scaling effects were chosen for analysis, as the most noticeable. Scaling introduces a bias in the angle between reconstructed tracks, thus two different scenarios may take place: vertex position reconstruction bias (spacial errors are introduced in the vertex reconstruction) or missing vertex (reconstruction algorithm fails to reconstruct the vertex). As a result, reduced vertex reconstruction efficiency and increased spread in the spacial distribution of reconstructed vertices are expected [12].

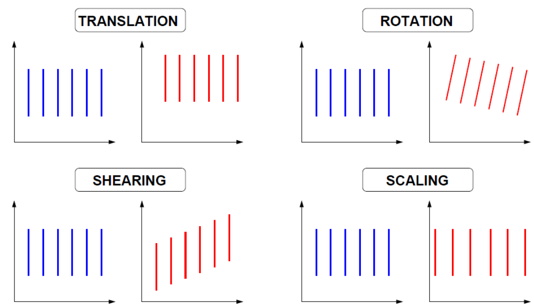

Figure 2: A schematic of the "weak modes" of the VELO [12]

3 Secondary vertices analysis

Precise knowledge of the position of the VELO is crucial for the detector to achieve best performance. To infer the exact location and detect possible unnoticed scaling effects a 2D map of the detector using secondary vertices of interaction with the VELO material was created. In order to reconstruct a complete map of the detector, the beam-gas Monte Carlo events were simulated, 2200 events for MC truth vertices and 9600 for reconstructed vertices. Created runs mimic the injection of helium or neon gas into the beam crossing region, providing a number of collisions distributed throughout the VELO.

Events were generated and analysed through the following software chain:

- Gauss: Generation of the physical process and interactions of produced particles with the detector;
- Boole: Digitization of the detector response;
- Brunel: Software reconstruction of the events from detector readout to reconstructed object as tracks and vertices;
- Bender: Analysis of tracks and vertices properties (e.g. vertices positions), stored in a ROOT file.

The information stored in the ROOT file were then analyzed by a C++ macro.

3.1 2D maps and vertices selection

Vertices positions in the detector, which layout can be seen in Figure 3, stored in the ROOT file created by Bender were analysed using the C++ macro, creating detailed maps of the VELO on different planes, shown in Figures 4, 5 and 6 for the MC truth vertices and Figures 7 and 8 for the reconstructed vertices. The maps contain vertices arising from the beam collisions with the gas and the RF foil wrapped around the modules. Only the interactions with the sensors carry useful information, thus the radial cut greater than 1 mm from the beamline was applied. The effect of it can be observed in Figures 4c and 4d and Figures 5b and 5d. With this, the maps contained only the vertices arising from the material interactions with the sensors. In the following section, the histograms for MC vertices positions for 2200 generated events and reconstructed vertices positions for 9600 generated events are shown. The number of events for the reconstruction process was greater than for the case of true MC vertices because of the difference of the Computing Grid response to the algorithms used in the creation of both datasets, which seemed to be more error prone for the true MC vertices.

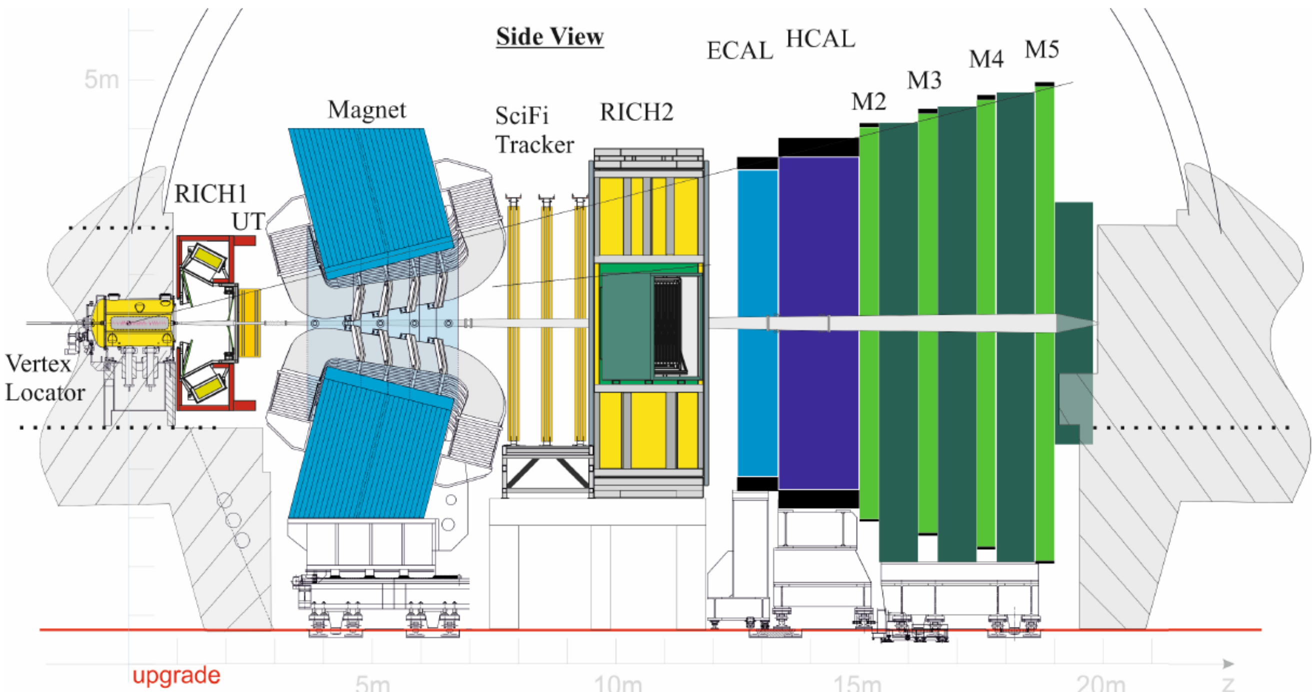

Figure 3: Schematic side-view of the Upgrade II detector [7]

3.2 MC vertices positions plots for 2200 events

Comparing the Figure 4 with the detector layout in Figure 3, one can see that the "black" bands are showing beam pipe, magnet, TT tracking stations and the VELO modules.

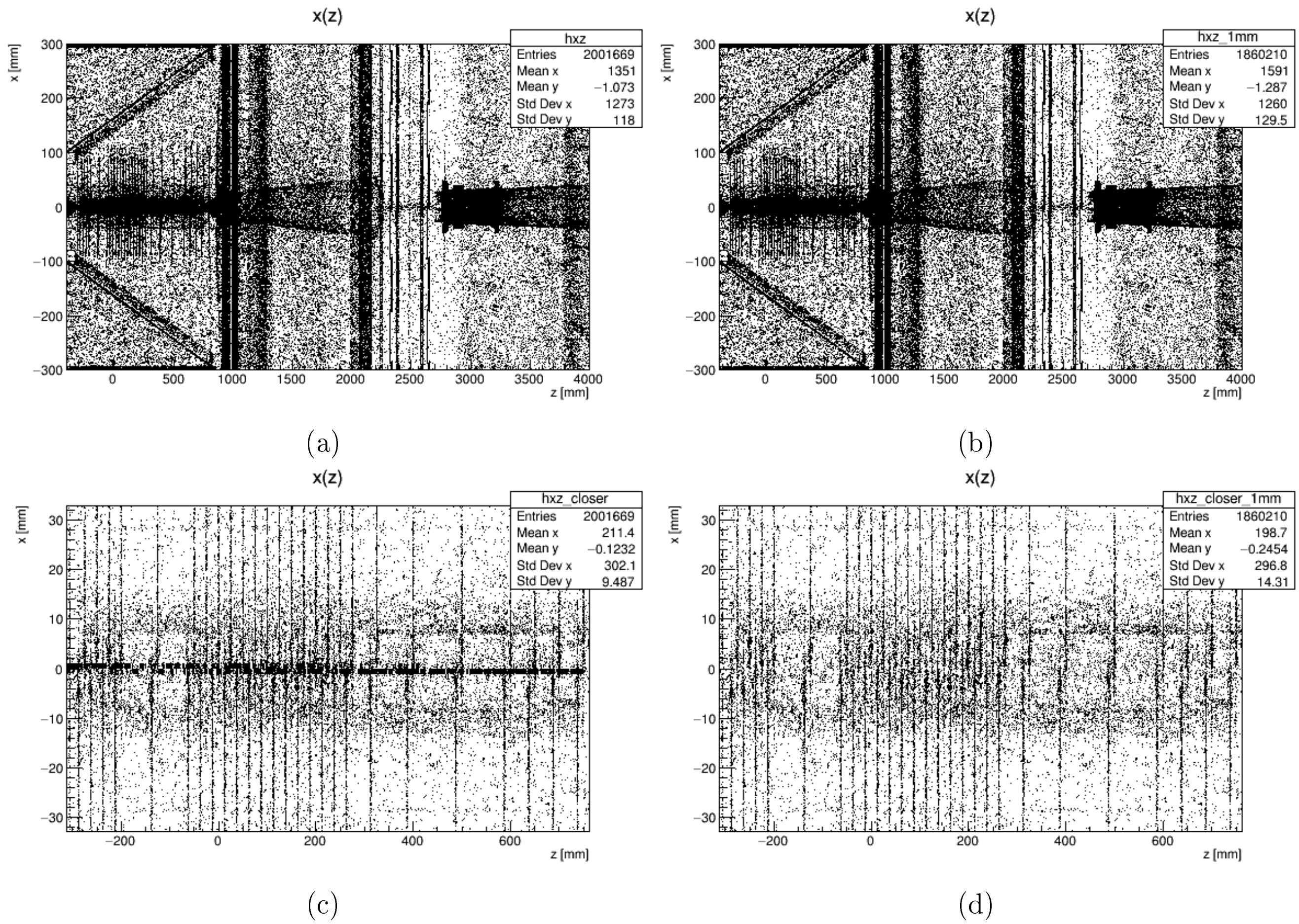

Figure 4: x(z) plane for MC vertices positions plots for 2200 events:
(a) x(z);
(b) x(z) with a radial cut for PV position ≥ 1mm from z axis;
(c) x(z) - close-up on VELO modules;
(d) x(z) - close-up on VELO modules, with a radial cut for PV position ≥ 1mm from z axis.

Taking a look into the plane perpendicular to the beamline shown in Fig. 5, the shape of the modules can be distinguished from a mesh of points corresponding to the secondary vertices positions. In Figures 5a and 5b one can see also the module support. In Figures 5c and 5d one can distinguish the RF foil that acts as LHC beam pipe in the VELO region.

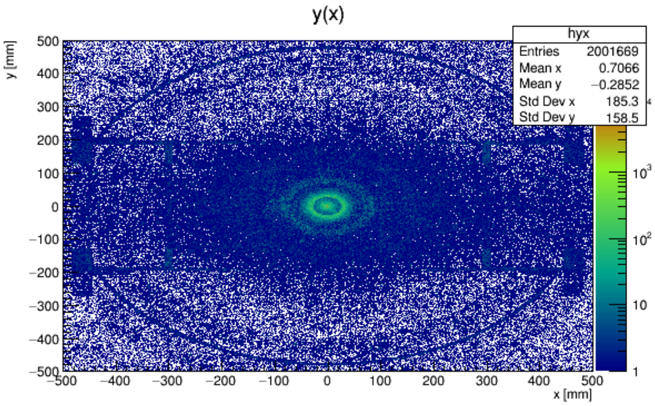

(a)

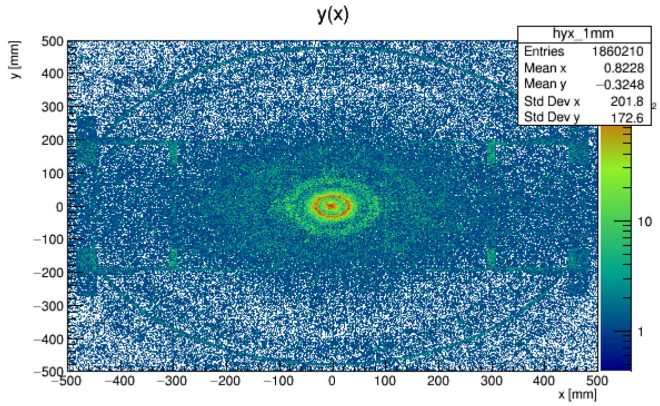

(b)

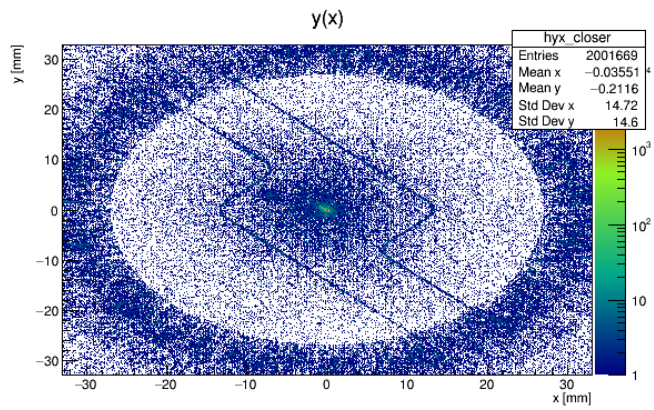

(c)

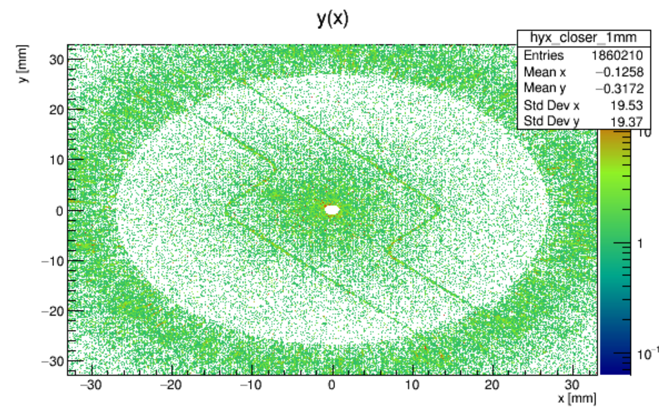

(d)

Figure 5: y(x) plane for MC vertices positions plots for 2200 events:
(a) y(x);
(b) y(x) with a radial cut for PV position $\geq$ 1mm from z axis;
(c) y(x) - close-up on VELO modules;
(d) y(x) - close-up on VELO modules, with a radial cut for PV position $\geq$ 1mm from z axis.

One can extract a module position by plotting the PV distribution around its z position, two examples are shown in Fig. 6a and Fig. 6b for module number 1, located at $z = -275$ mm, and module number 17, located at $z = 25.0$ mm.

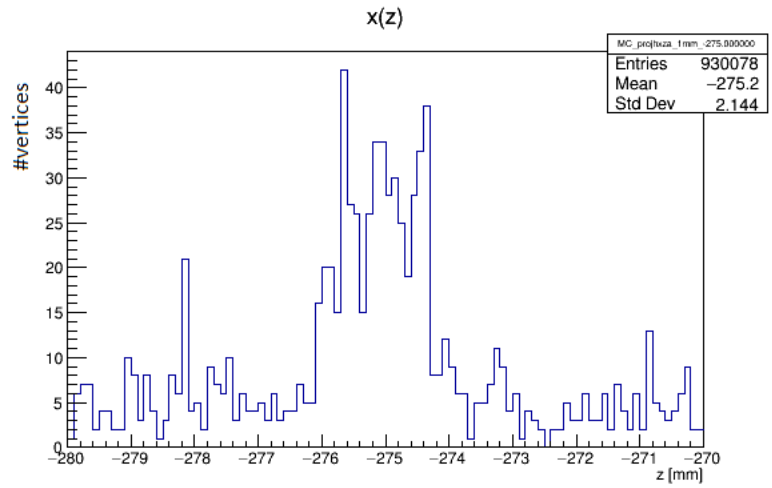

(a)

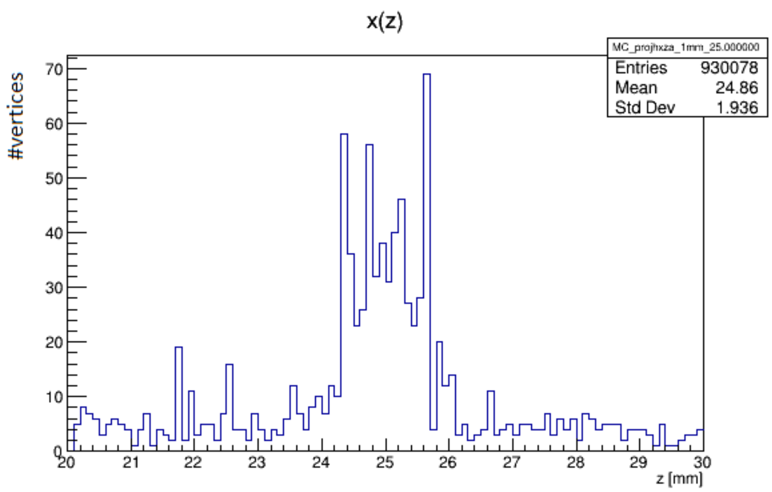

(b)

Figure 6: x(z) plane, A side and corresponding projections for MC vertices positions plots for 2200 events:
(a) Projection on z axis for the first module (-275.0 mm);
(b) Projection on z axis for one of the middle modules (25.0 mm).

3.3 Reconstructed vertices positions plots for 9600 events

The configuration of the PV algorithms was optimized to reconstruct PV with higher efficiency, as consequence the secondary vertices are rejected in the algorithm selection, as they are considered as the background. This is shown in Figure 7 and 8 where all reconstructed PV are plotted. One can see they are located only within 1 mm radial distance from the beamline.

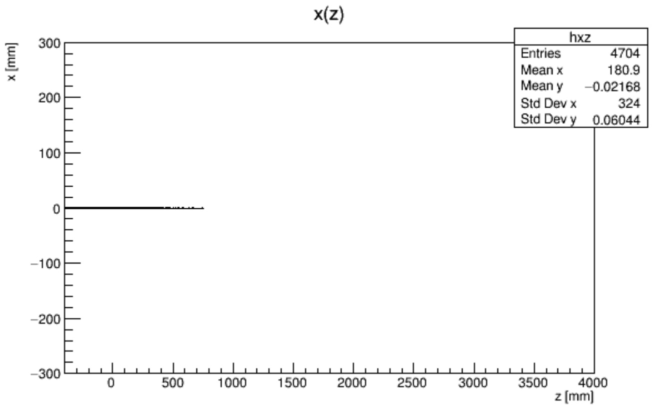

(a)

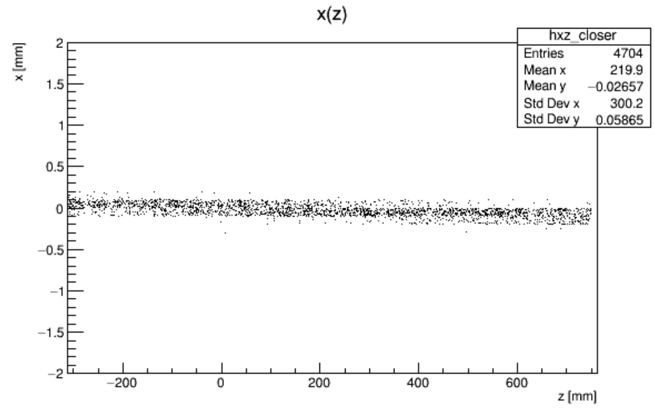

(b)

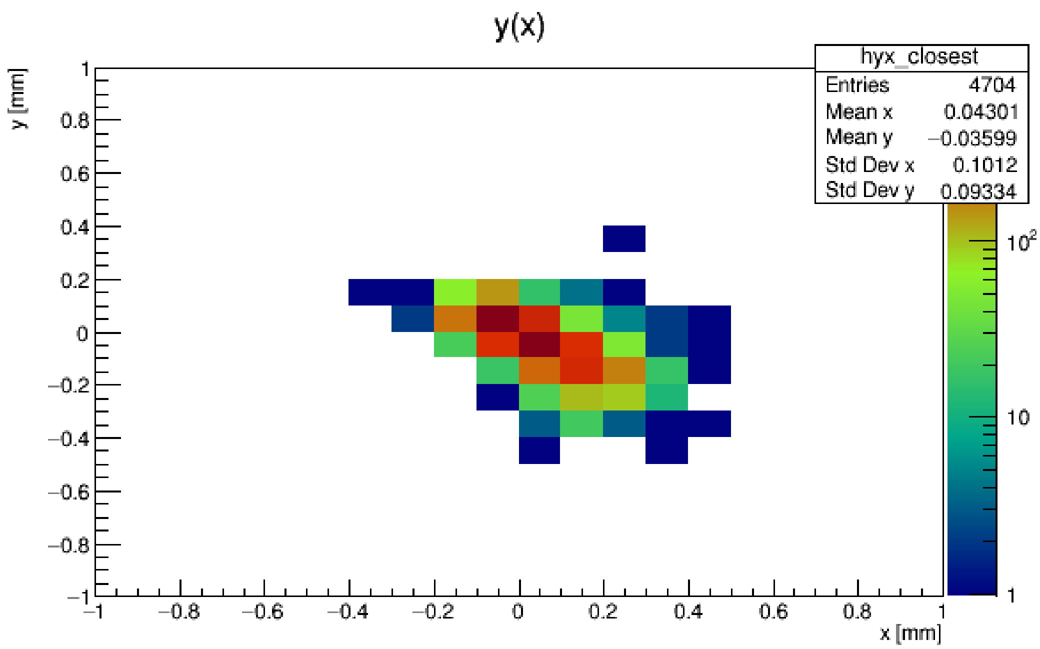

(c)

Figure 7: Reconstructed vertices positions plots for 9600 events:
(a) x(z);
(b) x(z) - close-up on VELO modules;
(c) y(x) - close-up on VELO modules.

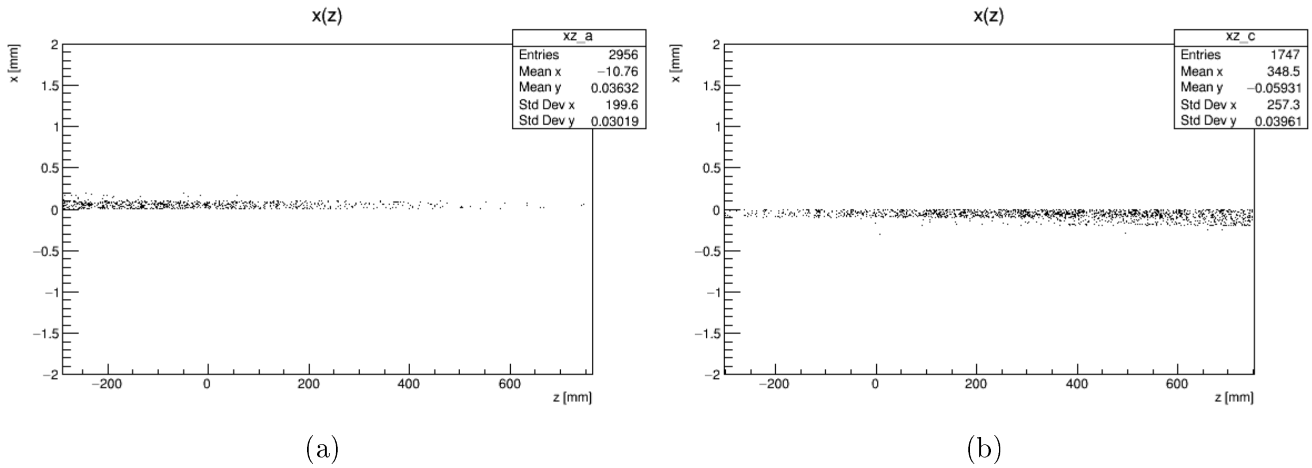

Figure 8: x(z) plane, both sides of modules, for reconstructed vertices positions and 9600 events:
(a) x(z) - A side of modules;
(b) x(z) - C side of modules.

4 Future work

The PV algorithm for this study should be properly configured in order to be able to reconstruct also secondary vertices. Having the distribution of the secondary vertex position, one can fit the histogram projections on z coordinate of the secondary vertex for each module and thus obtain their positions. One can compute the module position considering different misalignment scenario, e.g. z-scaling of the VELO. In this way we can evaluate the sensitivity of used method in the module position estimation.

References

[1] LHCb Collaboration. “The LHCb Detector at the LHC”. In: *JINST* **3** S08005 (2008).

[2] LHCb Collaboration. “LHCb detector performance”. In: *Int. J. Mod. Phys. A30* 1530022 [hep-ex/1412.6352] (2015).

[3] Alessio Piucci. “LHCb detector performance”. In: *J. Phys.: Conf. Ser.* 878 012012 (2017).

[4] Aaij R et al. (LHCb collaboration). In: *Phys. Rev. Lett. 111 101805 (Preprint 1307.5024)* (2013).

[5] Aaij R et al. (LHCb collaboration). In: *JHEP 02 104 (Preprint 1512.04442)* (2016).

[6] Aaij R et al. (LHCb collaboration). In: *Phys. Rev. Lett. 115 072001 (Preprint 1507.03414)* (2015).

[7] LHCb Collaboration. “Physics case for an LHCb Upgrade II. Opportunities in flavour physics, and beyond, in the HL-LHC era”. In: CERN-LHCC-2018-027 LHCB-PUB-2018-009 (2018).

[8] Aaij R et al. (LHCb collaboration). In: *Eur. Phys. J. C73: 2373 (Preprint* hep-ph/0506026*)* (2013).

[9] LHCb collaboration. “LHCb Tracker Upgrade Technical Design Report”. In: *CERN/LHCC 2014-001 LHCb TDR 15* (2014).

[10] W. D. Hulsbergen. “The global covariance matrix of tracks fitted with a Kalman filter and an application in detector alignment”. In: arXiv:0810.2241v2 [physics.ins-det] (2008).

[11] J. Amoraal et al. “Application of vertex and mass constraints in track-based alignment”. In: *Nucl. Instrum. Methods Phys. Res. A* 712 48-55 (2013).

[12] S. Viret, C. Parkes, M. Gersabeck. “Alignment procedure of the LHCb Vertex Detector”. In: arXiv:0807.5067v1 [physics.ins-det] (2008).